

Fast terminal sliding mode tracking control of nonlinear uncertain mass–spring system with experimental verifications

Saeed Amirkhani¹, Saleh Mobayen², Nahal Iliiae²,
Olfa Boubaker³ and S Hassan Hosseinnia⁴

Abstract

In this article, a fast terminal sliding mode control technique is used for robust tracking control of a nonlinear uncertain mass–spring system in the existence of external perturbation. This system is considered as a benchmark problem in the flexible joint mechanisms. The joints flexibility in the robotic systems creates one of the most significant sources of parametric uncertainties. The theory of Lyapunov stability is used for the formulation of the proposed control method, and the presence of the sliding around the switching surface is satisfied in the finite time. Simulation results as well as the experimental verifications prove the efficiency and applicability of the suggested approach in the presence of parametric uncertainty, noise, and exterior disturbance.

Keywords

Nonlinear mass–spring system, fast terminal sliding mode, Lyapunov theory, finite time convergence, uncertainties

Date received: 2 October 2018; accepted: 2 January 2019

Topic: Robot Manipulation and Control

Topic Editor: Andrey V Savkin

Associate Editor: Giuseppe Carbone

Introduction

The position control of the nonlinear second-order systems is one of the principal issues in the fields of control engineering, mechanics, and robotics.^{1–3} Modeling of various industrial systems leads to second-order nonlinear equations. In addition, many complex systems have second-order nonlinear benchmark structures, which are used to develop new control strategies.⁴ In most of the applied problems, besides the nonlinearity of the control system, the parametric uncertainties, external disturbances, and measurement noises also existed, where these factors are studied in the benchmark systems for the development of robust control strategies.⁵ To test the novel control techniques, various benchmark control systems, such as inverted pendulum, ball and beam, magnetic levitation, and

mass–spring damper, have been employed. The nonlinear mass–spring system is considered as a benchmark problem in the flexible joint mechanisms.^{6,7} In the recent years,

¹ Department of Mechanical Engineering, University of Guilan, Rasht, Iran

² Advanced Control Systems Laboratory, Department of Electrical Engineering, University of Zanjan, Zanjan, Iran

³ University of Carthage, National Institute of Applied Sciences and Technology, Tunis, Tunisia

⁴ Department of Precision and Micro System Engineering, Delft University of Technology, Delft, The Netherlands

Corresponding author:

Saleh Mobayen, Advanced Control Systems Laboratory, Department of Electrical Engineering, University of Zanjan, P.O. Box 38791-45371, Zanjan, Iran.

Email: mobayen@znu.ac.ir



Creative Commons CC BY: This article is distributed under the terms of the Creative Commons Attribution 4.0 License

(<http://www.creativecommons.org/licenses/by/4.0/>) which permits any use, reproduction and distribution of the work without further permission provided the original work is attributed as specified on the SAGE and Open Access pages (<https://us.sagepub.com/en-us/nam/open-access-at-sage>).

considerable attention has been paid to the robotic manipulators with joint flexibilities, making it a significant issue.⁸ Robotic systems with flexible joints have been developed for safe and compatible interaction to sensitive spaces such as human environments.⁹ This class of robotic systems has been employed for the needs of accurate industrial automation. In fact, flexibility of the joints in the robotic manipulators is an important issue in some applications such as space manipulators,¹⁰ surgical robots,¹¹ human robots,¹² and industrial manipulators.¹³ A trajectory tracker based on model-reference adaptive control method has been proposed by Ulrich and Sasiadek¹⁰ for space manipulator with parametric uncertainties and elastic vibrations in the joints. In the study by Xiong et al.,¹⁴ a weighted path-planning technique is presented for a light-weight robot, where an interaction is carried out with the environment using the impedance control approach. Flexibility is an undesirable feature in flexible joint mechanisms due to causing serious control problems such as vibration, nonlinearity, coupling, and uncertainty.¹⁵ In the past years, various control strategies such as adaptive control based on Lyapunov theory,^{16,17} model predictive control method,¹⁸ switched fuzzy output-feedback control,¹⁹ neural network control,²⁰ feedforward control,²¹ vibration control based on passivity theory,²² and sliding mode control (SMC)²³ have been investigated for the control/tracking of mass-spring systems.

SMC method is an effective nonlinear control strategy that has been utilized in control of various linear and nonlinear systems.^{24–26} Sliding mode controllers, due to the fast transient response, simplicity in use, and strong robustness against external disturbances and uncertainties, are applied in various practical systems like automobiles,²⁷ aircrafts,²⁸ missile guidance,²⁹ satellites,³⁰ cryptosystems,³¹ power systems,³² and robotics manipulators.³³ About the sliding mode controllers, one of the significant drawbacks is that they do not guarantee the robustness in the reaching phase. In fact, robustness of SMCs is related to sliding phase, which they do not have robust performance until they reach to the sliding phase. As a result, the system can become unstable due to external disturbances.^{34,35} Moreover, there are some high-frequency oscillations in the form of chattering during the sliding phase, which have damaging effects on the actuators. However, much effort has been made to attain the convergence in the finite time, as well as to eliminate chattering in the SMC controllers.^{36,37} The result of these efforts is the development of the Terminal Sliding Mode Control (TSMC) method, which has finite-time convergence tracking error.³⁸ In addition to stabilization in the finite time, the TSMC technique has a high speed and robustness to the typical SMC, which attracts the attention of many control systems designers.^{37,39} However, because of the fractional powers and their derivatives, TSMC suffers from the singularity problem and cannot provide the tracking errors convergence when the system states reach zero.^{40,41} To eliminate

the constraints of TSMC, another type of controller has been introduced by Yu and Man⁴² which is called the Fast Terminal Sliding Mode Control (FTSMC). This type of controller, even when the states of system are not near the equilibrium point, has a fast convergence. In fact, FTSMC provides the strong robustness and fast convergence performance in the transient and steady-state conditions.⁴³ Therefore, in recent years, the use of this type of controller has attracted many researchers.^{44,45}

In the study by Erenturk,⁴⁶ the optimized PID and sliding mode controllers combined with a grey estimator are developed for the nonlinear two-mass spring system. In the study by Pai,⁴⁷ for multimode flexible systems, a robust input shaping control scheme is proposed via the neuro-sliding mode feedback controller. In Mamani et al.'s study,⁴⁸ the SMC scheme is employed for the robust position tracking control of a light single-link flexible robotic arm without considering the bounding limits on parametric uncertainties. In the study by Dong and Tang,⁴⁹ a SMC by adaptive backstepping approach is proposed for the control of flexible ball screw drives in the presence of exterior disturbances and time-varying parameter uncertainties. In Zouari et al.'s study,⁵⁰ the proportional-integral and sliding mode controllers are designed for robotic manipulator with uncertain flexible joint and all parts of manipulator containing actuators are modeled to obtain high performance. The sliding mode-based discrete Fourier transform is presented by Shitole and Sumathi⁵¹ for estimation of single-link flexible manipulators vibration mode. In the study by Zhang et al.,⁵² an adaptive smooth sliding mode technique for vibration control in modal space is proposed in the flexible manipulators with parallel structure and multiple smart linkages. The SMC method based on passivity theory is investigated by Chenarani and Binazadeh⁵³ for the control of uncertain nonlinear systems with flexible structure. Rsetam et al.⁵⁴ suggested a hierarchical non-singular terminal SMC technique for a single-link robotic arm with flexible joint. The problem of the sliding mode boundary control based on adaptive neural network with radial basis function scheme is studied by Yang and Tan⁵⁵ for a flexible single-link manipulator. To the authors' knowledge, heretofore no finite-time control scheme has been considered to use a novel FTSMC method for the robust position tracking control of nonlinear mass-spring system with Coulomb friction, time-variant external disturbance, parametric uncertainty, and measurement noise. The novel FTSMC approach has been employed for the system stability analysis and control system. The controller is designed such that fulfills the presence of the sliding in the vicinity of the switching surface in the finite time according to the Lyapunov stability theorem.

The organization of this article is denoted as follows: the second section depicts the description of the nonlinear uncertain mass-spring system. The third section proposes the fast terminal sliding manifold and the stability analysis of the finite-time FTSMC approach. In the fourth section,

the results of simulation on the nonlinear mass–spring system are provided. The fifth section presents experimental verifications on the practical mass–spring system which confirms the efficiency of the suggested method. Finally, conclusions of the study are given in the sixth section.

System modeling and problem definition

The nonlinear mass–spring system can be considered as

$$m\ddot{x}(t) + kx(t) + \mu mg \operatorname{sgn}(\dot{x}(t)) = -ku(t) \quad (1)$$

where $x(t)$ is the mass position, $u(t)$ signifies the system input, k represents the spring coefficient, g indicates the gravitational constant, m specifies the mass value, μ denotes the friction coefficient, and $\operatorname{sgn}(\cdot)$ is the sign function. The parametric uncertainties should be considered in modeling of practical systems, such as robotic manipulators, flexible joint mechanisms, and mobile robots. A robotic manipulator with flexible joint can be used for moving different masses. In our benchmark problem (mass–spring system), the parametric uncertainties in the experimental results have been considered as the variations of cart mass.

Considering the uncertainties and disturbances, the nonlinear mass–spring system (1) in the state-space form can be represented by

$$\begin{aligned} \dot{x}_1(t) &= x_2(t) \\ \dot{x}_2(t) &= f(x_1(t), x_2(t)) + \Delta f(x_1(t), x_2(t)) - \frac{k}{m}u(t) + d(t) \end{aligned} \quad (2)$$

where $f(x_1(t), x_2(t)) = -\frac{k}{m}x_1(t) - \mu g \operatorname{sgn}(x_2(t))$, $x_1(t)$ and $x_2(t)$ are the system states, the nonlinear functions $\Delta f(x_1(t), x_2(t))$ and $d(t)$ present the parametric uncertainties and external disturbances, respectively. The nonlinear uncertain mass–spring system (2) is expected to follow the reference trajectories $x_{1d}(t)$ and $x_{2d}(t)$ with $\dot{x}_{1d}(t) = x_{2d}(t)$.

Assumption 1. The perturbation terms $d(t)$, $\dot{d}(t)$, $\Delta f(x_1(t), x_2(t))$ and $\Delta \dot{f}(x_1(t), x_2(t))$ are norm bounded.

Define the tracking errors as

$$\begin{aligned} e_1(t) &= x_1(t) - x_{1d}(t), \\ e_2(t) &= x_2(t) - x_{2d}(t), \end{aligned} \quad (3)$$

where $\dot{e}_1(t) = e_2(t)$.

Lemma 1. Let the positive-definite Lyapunov functional guarantees the following differential inequality for $t \geq t_0$ and $V(t_0) \geq 0$ ⁵⁶

$$\dot{V}(t) \leq -\alpha V(t) - \beta V(t)^\eta \quad (4)$$

with α and β as two positive scalars and η ($0 < \eta < 1$) as a ratio of two odd positive integers. As a result, $V(t)$ converges to the origin (at least) in the finite time as

$$t_s = t_0 + \frac{1}{\alpha(1-\eta)} \ln \frac{\alpha V^{1-\eta}(t_0) + \beta}{\beta} \quad (5)$$

Main results

For the nonlinear uncertain mass–spring system, the sliding surface is described as

$$s(e_1, e_2) = c_1 e_1(t) + c_2 e_2(t) \quad (6)$$

where c_1 and c_2 ($c_2 \neq 0$) denote the gain constants. For guaranteeing the convergence of sliding surface (equation (6)) to the origin in the finite time, the fast terminal sliding manifold can be defined by

$$\sigma(s, \dot{s}) = \dot{s}(e_1, e_2) + \lambda s(e_1, e_2) + \mu s(e_1, e_2)^\eta \quad (7)$$

where λ and μ are two positive coefficients, and η ($1 > \eta > 0$) is the ratio of two odd positive integers.

In what follows, the finite-time convergence procedure of the recommended fast terminal sliding manifold to the equilibrium is guaranteed and the zero-tracking performance of the system states is fulfilled.

Theorem 1. Consider the nonlinear uncertain mass–spring system (equation (2)). The control law of the proposed FTSMC is considered as

$$\begin{aligned} \dot{u}(t) &= \frac{m}{kc_2} \left[c_1 \left(f(x_1(t), x_2(t)) - \dot{x}_{2d}(t) - \frac{k}{m}u(t) \right) \right. \\ &\quad + c_2 \left(\dot{f}(x_1(t), x_2(t)) - \ddot{x}_{2d}(t) \right) \\ &\quad + \kappa \operatorname{sgn}(\sigma(s, \dot{s})) |\sigma(s, \dot{s})|^\eta + \gamma \sigma(s, \dot{s}) + \chi \operatorname{sgn}(\sigma(s, \dot{s})) \\ &\quad + \left(c_1 e_2(t) + c_2 \left(f(x_1(t), x_2(t)) - \dot{x}_{2d}(t) - \frac{k}{m}u(t) \right) \right) \\ &\quad \left. \left(\lambda + \mu \eta s(e_1, e_2)^{\eta-1} \right) \right] \end{aligned} \quad (8)$$

where γ and κ are two positive constants and χ is a coefficient that satisfies

$$\begin{aligned} \chi &\geq \max \left(\left(c_1 + c_2 \left(\lambda + \mu \eta s(e_1, e_2)^{\eta-1} \right) \right) \left(\Delta f(x_1(t), x_2(t)) + d(t) \right) \right. \\ &\quad \left. + c_2 \left(\Delta \dot{f}(x_1(t), x_2(t)) + \dot{d}(t) \right) \right) \end{aligned} \quad (9)$$

Then, in the finite time, the proposed fast terminal sliding manifold (equation (7)) converges to zero, and the states of the nonlinear uncertain system follow the reference desired path.

Proof. From equations (2) and (3), the first and second derivatives of $e_2(t)$ are calculated as

$$\begin{aligned} \dot{e}_2(t) &= f(x_1(t), x_2(t)) + \Delta f(x_1(t), x_2(t)) - \dot{x}_{2d}(t) - \frac{k}{m}u(t) + d(t) \end{aligned} \quad (10)$$

$$\ddot{e}_2(t) = \dot{f}(x_1(t), x_2(t)) + \Delta \dot{f}(x_1(t), x_2(t)) - \frac{k}{m} \dot{u}(t) + \dot{d}(t) - \ddot{x}_{2d}(t) \quad (11)$$

where using equations (10) and (11), time derivative of equation (7) is achieved as

$$\begin{aligned} \dot{\sigma}(s, \dot{s}) &= \ddot{s}(e_1, e_2) + \lambda \dot{s}(e_1, e_2) + \mu \eta \dot{s}(e_1, e_2) s(e_1, e_2)^{\eta-1} \\ &= c_1 \dot{e}_2(t) + c_2 \ddot{e}_2(t) + \left(c_1 e_2(t) + c_2 \dot{e}_2(t) \right) \left(\lambda + \mu \eta s(e_1, e_2)^{\eta-1} \right) \\ &= c_1 \left(f(x_1(t), x_2(t)) + \Delta f(x_1(t), x_2(t)) - \dot{x}_{2d}(t) - \frac{k}{m} u(t) + d(t) \right) \\ &\quad + c_2 \left(\dot{f}(x_1(t), x_2(t)) + \Delta \dot{f}(x_1(t), x_2(t)) + \dot{d}(t) - \ddot{x}_{2d}(t) \right) - \frac{kc_2}{m} \dot{u}(t) \\ &\quad + \left(c_1 e_2(t) + c_2 \left(f(x_1(t), x_2(t)) + \Delta f(x_1(t), x_2(t)) - \dot{x}_{2d}(t) - \frac{k}{m} u(t) + d(t) \right) \right) \left(\lambda + \mu \eta s(e_1, e_2)^{\eta-1} \right) \end{aligned} \quad (12)$$

Now, construct the Lyapunov candidate functional as

$$V(\sigma(s, \dot{s})) = 0.5 \sigma(s, \dot{s})^2 \quad (13)$$

Differentiating the Lyapunov functional (13) and using equation (12), we obtain

$$\begin{aligned} \dot{V}(\sigma(s, \dot{s})) &= \sigma(s, \dot{s}) \dot{\sigma}(s, \dot{s}) \\ &= \sigma(s, \dot{s}) \left\{ c_1 \left(f(x_1(t), x_2(t)) - \dot{x}_{2d}(t) - \frac{k}{m} u(t) \right) + c_2 \left(\dot{f}(x_1(t), x_2(t)) - \ddot{x}_{2d}(t) \right) \right. \\ &\quad + \left(c_1 e_2(t) + c_2 \left(f(x_1(t), x_2(t)) - \dot{x}_{2d}(t) - \frac{k}{m} u(t) \right) \right) \left(\lambda + \mu \eta s(e_1, e_2)^{\eta-1} \right) - \frac{kc_2}{m} \dot{u}(t) \\ &\quad \left. + \left(c_1 + c_2 \left(\lambda + \mu \eta s(e_1, e_2)^{\eta-1} \right) \right) \left(\Delta f(x_1(t), x_2(t)) + d(t) \right) + c_2 \left(\Delta \dot{f}(x_1(t), x_2(t)) + \dot{d}(t) \right) \right\} \end{aligned} \quad (14)$$

where substituting equation (8) into equation (14), it yields

$$\begin{aligned} \dot{V}(\sigma(s, \dot{s})) &= -\kappa |\sigma(s, \dot{s})|^{\eta+1} - \gamma \sigma(s, \dot{s})^2 - \chi |\sigma(s, \dot{s})| \\ &\quad + \left(\left(c_1 + c_2 \left(\lambda + \mu \eta s(e_1, e_2)^{\eta-1} \right) \right) \left(\Delta f(x_1(t), x_2(t)) + d(t) \right) + c_2 \left(\Delta \dot{f}(x_1(t), x_2(t)) + \dot{d}(t) \right) \right) \sigma(s, \dot{s}) \end{aligned} \quad (15)$$

Consequently, from equations (9), (13), and (15) and using Lemma 1, we have

$$\dot{V}(\sigma(s, \dot{s})) \leq -\gamma \sigma(s, \dot{s})^2 - \kappa |\sigma(s, \dot{s})|^{\eta+1} \leq -\alpha V(\sigma(s, \dot{s})) - \beta V(\sigma(s, \dot{s}))^{\bar{\eta}} \quad (16)$$

with $\alpha = 2\gamma > 0$, $\beta = (2^{\bar{\eta}})\kappa > 0$, and $0 < \bar{\eta} = \frac{\eta+1}{2} < 1$. Then, the Lyapunov functional (13) decreases gradually, and the fast terminal sliding manifold (equation (7)) is convergent to the origin in the finite time. \square

Simulation results

To prove the theoretical results of the proposed controller, in this section, a mass-spring system is simulated. The mass-spring system with Coulomb friction is introduced as a benchmark problem in robotic systems with flexible mechanisms. This system can be employed to evaluate different control techniques to make it more effective for other complex flexible structures. The dynamic behavior of the nonlinear mass-spring system shown in Figure 1 can be defined by the following differential equations

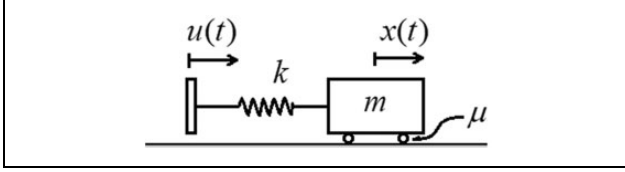


Figure 1. Schematic configuration of mass–spring system.

$$\begin{aligned}\dot{x}_1(t) &= x_2(t) \\ \dot{x}_2(t) &= -\frac{k}{m}x_1(t) - \mu g \operatorname{sgn}(x_2(t)) - \frac{k}{m}u(t)\end{aligned}\quad (17)$$

with

$$m = m_c + \frac{1}{3}m_s \quad (18)$$

$$\mu = \begin{cases} \mu_s & \dot{x}(t) = 0 \\ \mu_k & \dot{x}(t) \neq 0 \end{cases} \quad (19)$$

where $x_1(t)$ denotes the mass position, $x_2(t)$ signifies mass velocity, μ specifies Coulomb friction coefficient (with μ_s for static friction and μ_k for kinetic friction), g represents the gravity constant, m_s indicates the spring mass, and m_c is the cart mass. The initial conditions are considered as $x(0) = [0, 0]^T$. In these simulations, the following constant parameters are used in the nonlinear mass–spring system

$$m_s = 0.260\text{kg}, m_c = 0.850\text{kg}, k = 177\text{N/m}, g = 9.8\text{m/s}^2, \mu_s = 0.24, \mu_k = 0.11$$

Because the spring's mass is considerable in comparison with the cart mass, one-third of the spring's mass is added to the cart mass to diminish the effects of unmodeled nonlinear dynamics related to the spring.⁵⁷ Moreover, the coefficients of the static and dynamic friction are obtained via experimental test. The external disturbance is presumed as $d(t) = 5\sin(\pi t)\text{N}$, which is applied after 20 s. The sampling time is determined as 0.01 s. A sinusoidal input with 1 rad/s frequency and 2 cm amplitude is considered as the desired trajectory. The controller constant coefficients are given as $c_1 = 1$, $c_2 = 0.05$, $\lambda = 10$, $\kappa = 2.5$, $\gamma = 5.5$, $\ell = 1.5$, and $\beta = 2$. To figure out the proposed controller performance, a comparison with the PID controller has been made. The PID coefficients are determined by trial and error as $k_p = 7$, $k_i = 30$, and $k_d = 0.1$, and the employed controller for comparison purpose is considered as

$$u(t) = 7e_1(t) + 0.1e_2(t) + 30 \int_0^t e_1(\tau) d\tau.$$

It is concluded from simulation results that the mass–spring system state trajectories can successfully track the reference desired path through the proposed method. Figure 2 illustrates the time histories of the position and velocity of mass–spring setup in noise-free condition. As

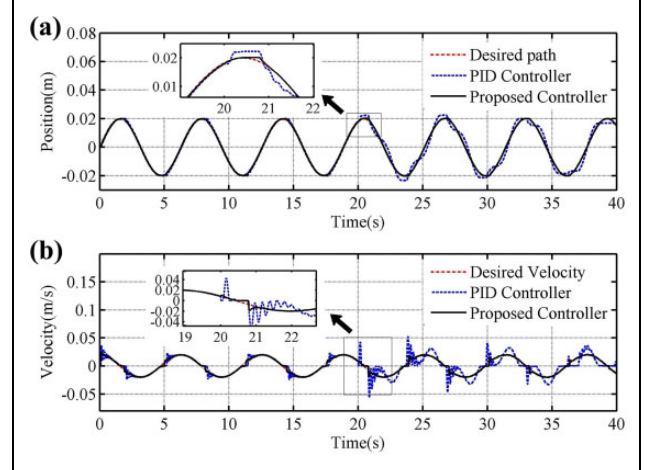


Figure 2. Simulation results of (a) position and (b) velocity of mass–spring system. PID: proportional–integral–derivative.

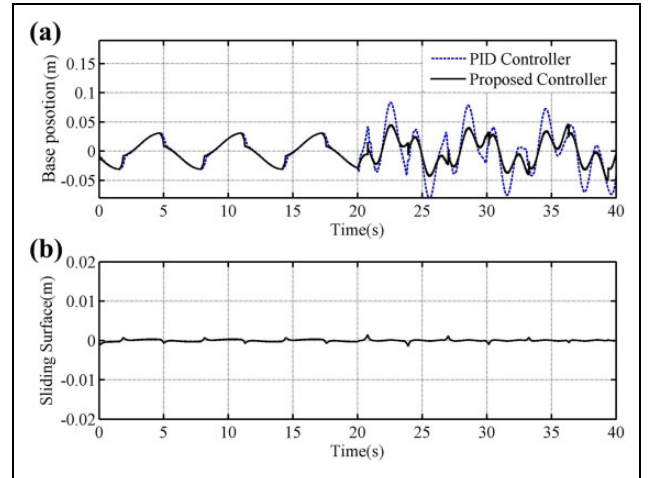


Figure 3. Time responses of (a) controllers' output and (b) sliding surface. PID: proportional–integral–derivative.

shown in Figure 2, in the presence of the external disturbance, the proposed controller has an acceptable performance rather than the other controller. Figure 3 demonstrates the time responses of the controllers' output and sliding surface. This figure exhibits that the output of the proposed controller has a fruitful performance and less control effort than the result of the PID controller.

To investigate the suggested control robustness, the noise effect and parametric uncertainty are also studied in simulations. For uncertainty term, we have added a coefficient of the Heaviside step function to the cart mass as $1.5H(t - 20)$. A Gaussian measurement noise is applied with zero-mean and variance of 0.2, amplitude of 0.001, and sampling time of 0.01 s. Figure 4 shows the position and velocity of mass–spring system in noisy condition. In the first 20 s, the system is only under the measurement noises. The external disturbance is applied after 20 s. It can be concluded from Figure 4 that the suggested FTSMC has

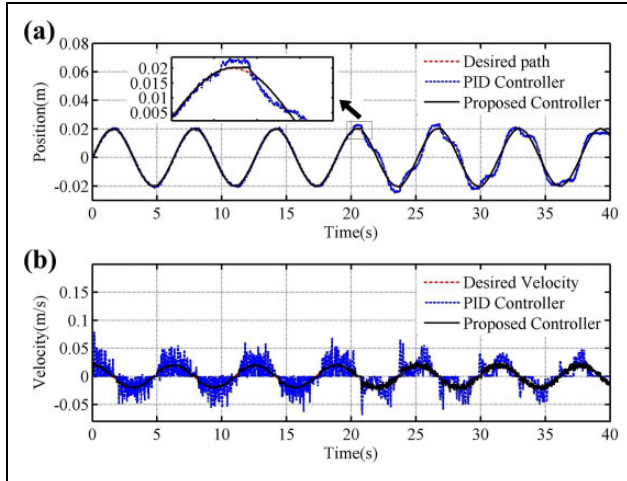


Figure 4. (a) Position and (b) velocity of mass-spring system in noisy condition. PID: proportional-integral-derivative.

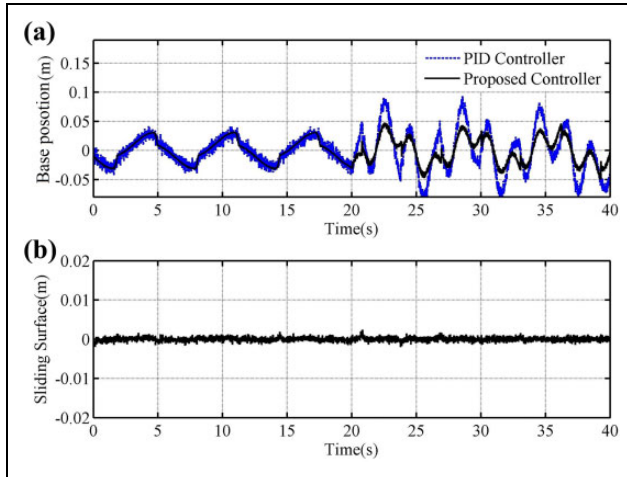


Figure 5. (a) Controllers' output and (b) sliding surface in noisy condition. PID: proportional-integral-derivative.

robust performance in noisy condition. Though derivative factor in the PID controller is negligible, the effect of measurement noise on the velocity plot (Figure 4(b)) is quite evident. Figure 5 illustrates the controllers' output and the proposed sliding surface. It can be found from Figure 5 that the output of the proposed controller has small oscillations, which confirms the superiority of the suggested scheme.

In the third part of simulations, to study the proposed controller performance to the parametric uncertainty, measurement noise, and the external disturbance, a sudden change also occurred in the amount of system's mass. At the moment of 20 s, a mass of 1.5 kg has been added to the system. Figures 6 and 7 depict the simulation results for the new condition. As it can be seen in Figure 6, the position and velocity of the mass through the proposed controller have robust behavior versus parametric variation. Furthermore, Figure 7 illustrates the increment in the amplitudes of the control output due to mass change.

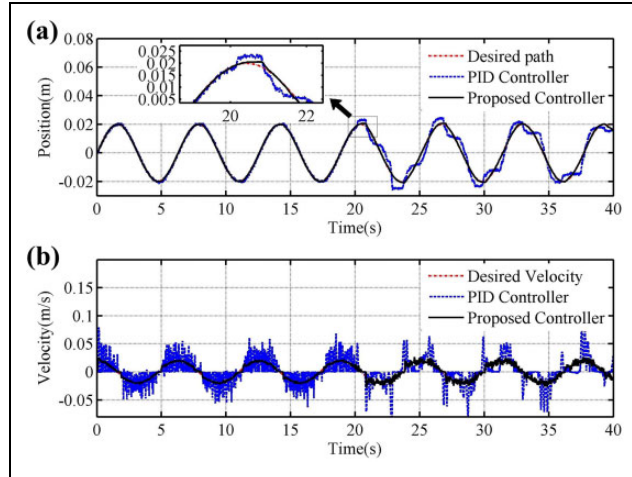


Figure 6. (a) Position and (b) velocity of mass-spring system in noisy condition under disturbance and mass uncertainty. PID: proportional-integral-derivative.

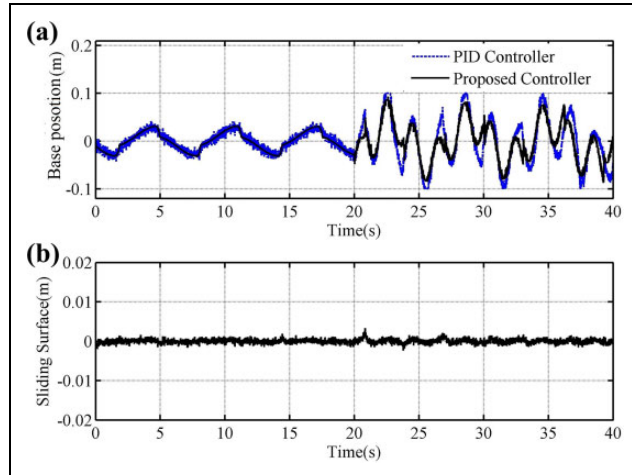


Figure 7. (a) Controllers' outputs and (b) sliding surface in noisy condition under disturbance and mass uncertainty. PID: proportional-integral-derivative.

As observed above, the obtained results of the simulations show that the proposed FTSMC technique has acceptable robust performance in the presence of the external disturbance, parametric uncertainty, and noisy condition.

Experimental results

In the following, the experimental results of the suggested control technique are presented via Matlab® [version R2016a] Simulink® software and Arduino® hardware support package toolbox. We have performed some experiments on the practical two-mass-spring system built in *Department of Electrical Engineering at University of Zanjan*. Figure 8 displays the built in two-mass-spring system. In this setup, two potentiometer position sensors measure the positions of carts (masses). One of the carts is considered as the base, which is excited through MG996 R (TowerPro) servomotor.

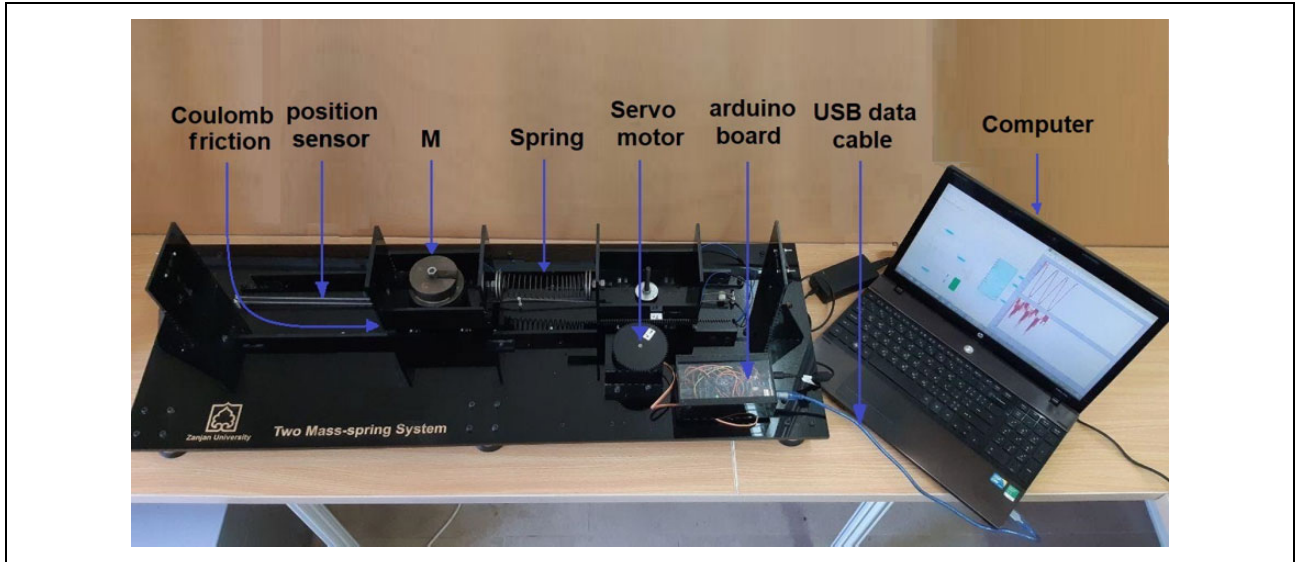


Figure 8. Built in mass–spring system.

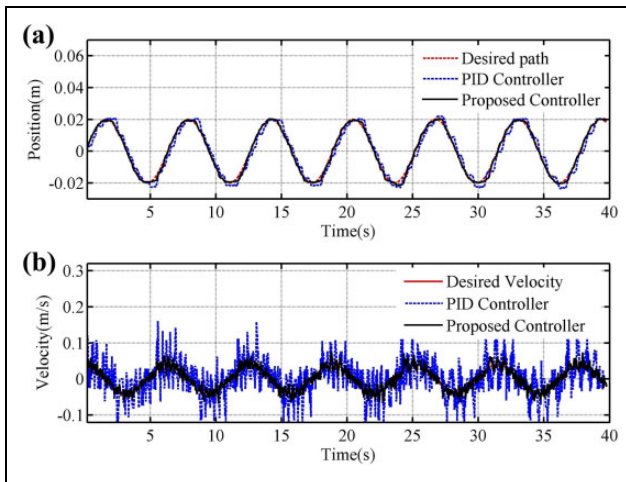


Figure 9. Experimental results of (a) position and (b) velocity of mass–spring system under mass uncertainty. PID: proportional–integral–derivative.

The Arduino MEGA 2560 board (based on the ATmega2560 microcontroller) has been used in the electronic part of the system. A computer with the specifications Intel® Core™ i3 2.40 GHz CPU and 3.00 GB RAM is employed to the control system and by considering 0.01 s for control loop sampling time and ode3 (Bogacki–Shampine) solver, control process of this system is completely real-time. The FTSMC and PID controllers are applied to position control of the mass on the reference trajectory as $x(t) = 0.02\sin t$. The initial values of position and velocity of the cart ($x_1(0)$ and $x_2(0)$) are zero. To study the robustness performance of the controllers versus the parametric uncertainties, a mass of 1.5 kg has been added to the cart mass after the moment $t = 20$ s.

The experimental results of position tracking and velocity of the cart mass are indicated in Figure 9. As can be

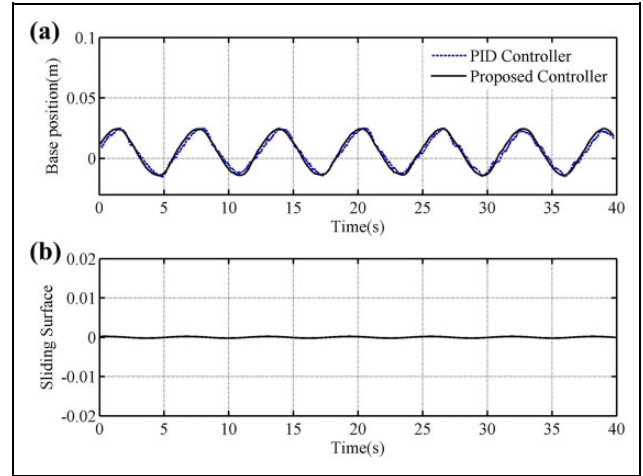


Figure 10. Experimental results of (a) control outputs and (b) sliding surface of built-in system. PID: proportional–integral–derivative.

observed in Figure 9(a), the proposed controller has a high accuracy in tracking of the desired path, even in the presence of mass uncertainties. Moreover, the oscillations of mass velocity are shown in Figure 9(b), which represents acceptable response of the suggested controller by considering the measurement noise.

Figure 10 demonstrates the outputs of the controllers and sliding surface of the proposed method. As can be seen from Figure 10(a), there are some differences between the control outputs in the simulation and experimental results. The main reason for the mentioned difference after the moment $t = 20$ s is related to the nonexistence of disturbance in the experimental results. The slight difference in the control outputs between the simulation and experimental results before the moment $t = 20$ s is because of the

un-modeled nonlinear dynamics in the simulated system. It can be concluded from Figure 10 that the output of the proposed control technique is more smooth than the control output of the other method, which confirms the advantage of the proposed approach.

Conclusions

In this article, the fast terminal SMC approach was investigated for robust tracking control problem of an uncertain nonlinear mass–spring system with parametric uncertainty, noise, and external disturbance. In this way, a new fast terminal sliding surface was presented and an original robust FTSMC procedure for the tracking purpose of the nonlinear uncertain mass–spring system (as a benchmark problem of flexible joint mechanisms) was proposed. Moreover, the convergence of the fast terminal sliding surface in finite time to the origin was studied via Lyapunov stability theorem. Lastly, the effectiveness and success of the recommended method were confirmed via simulation and experimental results on the nonlinear uncertain mass–spring system. It is worth mentioning that the proposed robust control approach can be employed for more complex higher order uncertain nonlinear systems, such as flexible joint mechanisms.

Declaration of conflicting interests

The author(s) declared no potential conflicts of interest with respect to the research, authorship, and/or publication of this article.

Funding

The author(s) received no financial support for the research, authorship, and/or publication of this article.

References

1. Mondal S and Mahanta C. Adaptive second order terminal sliding mode controller for robotic manipulators. *J Franklin Inst* 2014; 351: 2356–2377.
2. Savkin AV and Wang C. A simple biologically inspired algorithm for collision-free navigation of a unicycle-like robot in dynamic environments with moving obstacles. *Robotica* 2013; 31(2): 993–1001.
3. Mehdi H and Boubaker O. New robust tracking control for safe constrained robots under unknown impedance environment. In: *Conference towards autonomous robotic systems*, Bristol, UK, 20–23 August 2012, pp. 313–323. Bristol, UK: Springer.
4. Mehdi H and Boubaker O. Robust impedance control-based Lyapunov-Hamiltonian approach for constrained robots. *Int J Adv Robot Syst* 2015; 12: 190.
5. Mahmoud MS and Nasir MT. Robust control design of wheeled inverted pendulum assistant robot. *IEEE/CAA J Autom Sinica* 2017; 4(4): 628–638.
6. Ulrich S, Sasiadek JZ, and Barkana I. Nonlinear adaptive output feedback control of flexible-joint space manipulators with joint stiffness uncertainties. *J Guid Control Dyn* 2014; 37(6): 1961–1975.
7. Chaoui H and Gueaieb W. Type-2 fuzzy logic control of a flexible-joint manipulator. *J Intell Robot Syst* 2008; 51(2): 159–186.
8. Korayem M and Nekoo S. Finite-time state-dependent Riccati equation for time-varying nonaffine systems: rigid and flexible joint manipulator control. *ISA Trans* 2015; 54: 125–144.
9. Miranda-Colorado R, Aguilar LT, and Moreno-Valenzuela J. A model-based velocity controller for chaotization of flexible joint robot manipulators: synthesis, analysis, and experimental evaluations. *Int J Adv Robot Syst* 2018; 15: 1729881418802528.
10. Ulrich S and Sasiadek JZ. On the simple adaptive control of flexible-joint space manipulators with uncertainties. In: Sasiadek J (ed) *Aerospace Robotics II*. Cham, Switzerland: Springer, 2015, pp. 13–23.
11. Haraguchi D, Kanno T, Tadano K, et al. A pneumatically driven surgical manipulator with a flexible distal joint capable of force sensing. *IEEE/ASME Trans Mech* 2015; 20: 2950–2961.
12. Xiong GL, Chen HC, Zhang RH, et al. Control of human-robot interaction flexible joint lightweight manipulator based joint torque sensors. *Adv Mater Res* 2012; 403–408: 5022–5029.
13. Saupe F and Knobloch A. Experimental determination of frequency response function estimates for flexible joint industrial manipulators with serial kinematics. *Mech Syst Signal Process* 2015; 52: 60–72.
14. Xiong G, Chen H, Zhang R, et al. Robot-environment interaction control of a flexible joint light weight robot manipulator. *Int J Adv Robot Syst* 2012; 9: 76.
15. Dwivedy SK and Eberhard P. Dynamic analysis of flexible manipulators: a literature review. *Mech Mach Theory* 2006; 41(7): 749–777.
16. Dupree K, Liang C-H, Hu G, et al. Adaptive Lyapunov-based control of a robot and mass–spring system undergoing an impact collision. *IEEE Trans Syst Man Cybern B (Cybern)* 2008; 38(4): 1050–1061.
17. Mehdi H and Boubaker O. Stiffness and impedance control using Lyapunov theory for robot-aided rehabilitation. *Int J Social Robot* 2012; 4(suppl 1): 107–119.
18. Cairano SD, Bemporad A, Kolmanovsky IV, et al. Model predictive control of magnetically actuated mass spring dampers for automotive applications. *Int J Control* 2007; 80(11): 1701–1716.
19. Li H, Pan Y, Shi P, et al. Switched fuzzy output feedback control and its application to a mass–spring–damping system. *IEEE Trans Fuzzy Syst* 2016; 24: 1259–1269.
20. Sun C, He W, and Hong J. Neural network control of a flexible robotic manipulator using the lumped spring-mass model. *IEEE Trans Syst Man Cybern Syst* 2017; 47: 1863–1874.
21. Palmer LR III and Eaton CE. Periodic spring–mass running over uneven terrain through feedforward control of landing conditions. *Bioinspir Biomim* 2014; 9(3): 036018.

22. Aoki T, Yamashita Y, and Tsubakino D. Vibration suppression for mass-spring-damper systems with a tuned mass damper using interconnection and damping assignment passivity-based control. *Int J Robust Nonlinear Control* 2016; 26: 235–251.
23. Xing K, Huang J, He J, et al. Sliding mode tracking for actuators comprising pneumatic muscle and torsion spring. *Trans Inst Meas Control* 2012; 34: 255–277.
24. Incremona GP, Rubagotti M, and Ferrara A. Sliding mode control of constrained nonlinear systems. *IEEE Trans Autom Control* 2017; 62(6): 2965–2972.
25. Yang JM and Kim JH. Sliding mode control for trajectory tracking of nonholonomic wheeled mobile robots. *IEEE Trans Robot Autom* 1999; 15: 578–587.
26. Sarfraz M, Rehman Fu, and Shah I. Robust stabilizing control of nonholonomic systems with uncertainties via adaptive integral sliding mode: an underwater vehicle example. *Int J Adv Robot Syst* 2017; 14(7): 1729881417732693.
27. Wang H, Kong H, Man Z, et al. Sliding mode control for steer-by-wire systems with AC motors in road vehicles. *IEEE Trans Ind Electron* 2014; 61: 1596–1611.
28. Rao DV and Sinha NK. A sliding mode controller for aircraft simulated entry into spin. *Aerospace Sci Technol* 2013; 28(1): 154–163.
29. Wang Z. Adaptive smooth second-order sliding mode control method with application to missile guidance. *Trans Inst Meas Control* 2017; 39: 848–860.
30. Nair RR, Behera L, Kumar V, et al. Multisatellite formation control for remote sensing applications using artificial potential field and adaptive fuzzy sliding mode control. *IEEE Syst J* 2015; 9: 508–518.
31. Muthukumar P, Balasubramaniam P, and Ratnavelu K. Sliding mode control design for synchronization of fractional order chaotic systems and its application to a new cryptosystem. *Int J Dyn Control* 2017; 5: 115–123.
32. Liu J, Vazquez S, Wu L, et al. Extended state observer-based sliding-mode control for three-phase power converters. *IEEE Trans Ind Electron* 2017; 64: 22–31.
33. Baek J, Jin M, and Han S. A new adaptive sliding-mode control scheme for application to robot manipulators. *IEEE Trans Ind Electron* 2016; 63(6): 3628–3637.
34. Pisano A and Usai E. Sliding mode control: a survey with applications in math. *Math Comput Simul* 2011; 81: 954–979.
35. Mobayen S. Design of CNF-based nonlinear integral sliding surface for matched uncertain linear systems with multiple state-delays. *Nonlinear Dyn* 2014; 77: 1047–1054.
36. Wang H, Man Z, Kong H, et al. Design and implementation of adaptive terminal sliding-mode control on a steer-by-wire equipped road vehicle. *IEEE Trans Ind Electron* 2016; 63: 5774–5785.
37. Chen M, Wu Q-X, and Cui R-X. Terminal sliding mode tracking control for a class of SISO uncertain nonlinear systems. *ISA Trans* 2013; 52(2): 198–206.
38. Kamal S, Moreno JA, Chalanga A, et al. Continuous terminal sliding-mode controller. *Automation* 2016; 69: 308–314.
39. Yang J, Li S, Su J, et al. Continuous nonsingular terminal sliding mode control for systems with mismatched disturbances. *Automation* 2013; 49(7): 2287–2291.
40. Madani T, Daachi B, and Djouani K. Non-singular terminal sliding mode controller: application to an actuated exoskeleton. *Mechatron* 2016; 33: 136–145.
41. Su R, Zong Q, Tian B, et al. Comprehensive design of disturbance observer and non-singular terminal sliding mode control for reusable launch vehicles. *IET Control Theory Appl* 2015; 9: 1821–1830.
42. Yu X and Zhihong M. Fast terminal sliding-mode control design for nonlinear dynamical systems. *IEEE Trans Circuits Syst I Fundam Theory Appl* 2002; 49: 261–264.
43. Mobayen S. An adaptive fast terminal sliding mode control combined with global sliding mode scheme for tracking control of uncertain nonlinear third-order systems. *Nonlinear Dyn* 2015; 82: 599–610.
44. Van M, Ge SS, and Ren H. Finite time fault tolerant control for robot manipulators using time delay estimation and continuous nonsingular fast terminal sliding mode control. *IEEE Trans Cybern* 2017; 47: 1681–1693.
45. Mobayen S and Tchier F. Nonsingular fast terminal sliding-mode stabilizer for a class of uncertain nonlinear systems based on disturbance observer. *Sci Iran* 2017; 24(3): 1410–1418.
46. Erenturk K. Nonlinear two-mass system control with sliding-mode and optimised proportional–integral derivative controller combined with a grey estimator. *IET Control Theory Appl* 2008; 2(7): 635–642.
47. Pai MC. Robust input shaping control for multi-mode flexible structures using neuro-sliding mode output feedback control. *J Franklin Inst* 2012; 349: 1283–1303.
48. Mamani G, Becedas J, and Feliu V. Sliding mode tracking control of a very lightweight single-link flexible robot robust to payload changes and motor friction. *J Vib Control* 2012; 18: 1141–1155.
49. Dong L and Tang WC. Adaptive backstepping sliding mode control of flexible ball screw drives with time-varying parametric uncertainties and disturbances. *ISA Trans* 2014; 53: 110–116.
50. Zouari L, Abid H, and Abid M. Sliding mode and PI controllers for uncertain flexible joint manipulator. *Int J Autom Comput* 2015; 12(2): 117–124.
51. Shitole C and Sumathi P. Sliding DFT-based vibration mode estimator for single-link flexible manipulator. *IEEE/ASME Trans Mech* 2015; 20: 3249–3256.
52. Zhang Q, Li C, Zhang J, et al. Smooth adaptive sliding mode vibration control of a flexible parallel manipulator with multiple smart linkages in modal space. *J Sound Vib* 2017; 411: 1–19.
53. Chenarani H and Binazadeh T. Flexible structure control of unmatched uncertain nonlinear systems via passivity-based sliding mode technique. *Iran J Sci Technol Trans Electr Eng* 2017; 41(7): 1–11.
54. Rsetam K, Cao Z, and Man Z. Hierarchical non-singular terminal sliding mode controller for a single link flexible joint robot manipulator. In: *2017 IEEE 56th annual conference on*

- Decision and control (CDC)*, Melbourne, Victoria, Australia, 12–15 December 2017, pp. 6677–6682. United States: IEEE.
55. Yang H-J and Tan M. Sliding mode control for flexible-link manipulators based on adaptive neural networks. *Int J Autom Comput* 2018; 15(2): 239–248.
56. Moulay E and Perruquetti W. Finite time stability and stabilization of a class of continuous systems. *J Math Anal Appl* 2006; 323(2): 1430–1443.
57. Rao SS and Yap FF. *Mechanical vibrations*. Upper Saddle River: Prentice Hall, 2011.